REVIEW ARTICLE

Recent advances in antimony removal using carbon-based nanomaterials: A review

Xuemei Hu[1], Shijie You (✉)[2], Fang Li[1], Yanbiao Liu (✉)[1]

1 Textile Pollution Controlling Engineering Center of Ministry of Environmental Protection, College of Environmental Science and Engineering, Donghua University, Shanghai 201620, China

2 State Key Laboratory of Urban Water Resource and Environment, School of Environment, Harbin Institute of Technology, Harbin 150090, China

<table>
<tr><td valign="top" width="50%">

H I G H L I G H T S

- The synthesis and physicochemical properties of various CNMs are reviewed.
- Sb removal using carbon-based nano-adsorbents and membranes are summarized.
- Details on adsorption behavior and mechanisms of Sb uptake by CNMs are discussed.
- Challenges and future prospects for rational design of advanced CNMs are provided.

</td><td valign="top" width="50%">

G R A P H I C A B S T R A C T

</td></tr>
</table>
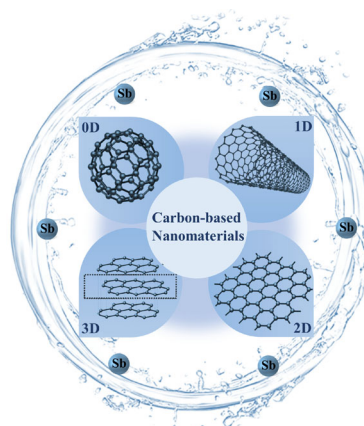
A B S T R A C T

Recently, special attention has been deserved to environmental risks of antimony (Sb) element that is of highly physiologic toxicity to human. Conventional coagulation and ion exchange methods for Sb removal are faced with challenges of low efficiency, high cost and secondary pollution. Adsorption based on carbon nanomaterials (CNMs; e.g., carbon nanotubes, graphene, graphene oxide, reduced graphene oxide and their derivatives) may provide effective alternative because the CNMs have high surface area, rich surface chemistry and high stability. In particular, good conductivity makes it possible to create linkage between adsorption and electrochemistry, thereby the synergistic interaction will be expected for enhanced Sb removal. This review article summarizes the state of art on Sb removal using CNMs with the form of nano-adsorbents and/or filtration membranes. In details, procedures of synthesis and functionalization of different forms of CNMs were reviewed. Next, adsorption behavior and the underlying mechanisms toward Sb removal using various CNMs were presented as resulting from a retrospective analysis of literatures. Last, we prospect the needs for mass production and regeneration of CNMs adsorbents using more affordable precursors and objective assessment of environmental impacts in future studies.

1   Introduction

With the inexorable industrialization and modern agricultural practices, a large number of heavy metal ions are discharged into water bodies, which inevitably exerts an adverse impact on water environment, aquatic ecosystem as well as human health (He et al., 2019; Boreiko and Rossman, 2020). Environmental risks associated with antimony (Sb) have attracted extensive attention in recent years (He et al., 2012; Leng et al., 2012). Sb pollution appears to be ubiquitous throughout various environmental mediums resulting from natural sources such as volcanic activity and anthropogenic activities like mining, coal combustion and agricultural production (He et al., 2012;

✉ Corresponding authors
E-mail: sjyou@hit.edu.cn (S. You); yanbiaoliu@dhu.edu.cn (Y. Liu)

He et al., 2019). Elevated Sb concentrations up to 7000 µg/L have been reported in a water body close to Sb mining and smelting areas (Xu et al., 2016). Exposure of humans or animals to Sb substances through oral, dermal or inhalation may pose serious adverse health effects such as nausea, vomiting, anorexia, abdominal pain, and stomach ulcers (Saerens et al., 2019; Boreiko and Rossman, 2020). Given their high toxicity, the European Union (EU) and the US Environmental Protection Agency (EPA) have listed Sb-containing compounds as the priority pollutants. The World Health Organization (WHO) has recommended the maximum concentration level (MCL) of total Sb (Sb_{total}) to be 5.0 µg/L in drinking water (Xi et al., 2015).

Compared with arsenic (As), less attention has been paid to the Sb removal, though they are in the same group in the periodic table. Several technologies such as coagulation and electrochemical method have been reported to be effective for Sb removal, but challenges remain associated with the use of chemicals, high energy consumption and the risk of secondary pollution (Du et al., 2014; Norra and Radjenovic, 2021). Despite the effectiveness, the ion exchange technique is faced with the difficulties of resin regeneration and high operational cost (Chen et al., 2020; Jiang et al., 2021). More recently, adsorption and membrane separation have been widely recognized as promising alternative techniques. The design of such techniques is very efficient due to their flexibility and simplicity, which are easy to operate and service (Leng et al., 2012; Liu et al., 2020a; Liu et al., 2020b).

For decades, carbon materials have been used in a prodigious number of applications (Deng et al., 2015; Yi et al., 2019; Zhou et al., 2020). Carbon-based nanomaterials (CNMs), such as carbon nanotubes (CNT), carbon nanofiber, graphene and its derivatives (e.g., graphene oxide (GO), and reduced graphene oxide (rGO)), are the representatives of the most common carbon-based nanoscale adsorbents. The abundant CNMs have the advantages of large surface area with excellent chemical stability. Hence, they normally have high adsorption capacity and are environmentally friendly (Salam and Mohamed, 2013; Ghasemzadeh et al., 2014; Gusain et al., 2020). Recent advances in carbon-based membranes may provide new opportunities for the abatement of Sb from water using the membrane filtration technology (Li et al., 2020; Hu et al., 2021). An increasing number of papers have been published over the years on the removal of Sb by CNMs (Yu et al., 2014; Luo et al., 2015). However, a systematic overview is still needed to summarize the recent advances in the CNMs for the adsorptive removal of Sb, which is the main topic of this review. The first part of the review discusses the physicochemical properties of the CNMs and their general applications. Next, we focus on the application of CNMs as the adsorbents and membrane materials for the removal of Sb in water. The last part of the review is focused on the challenges and prospects for the rational design of advanced functional CNMs with improved reactivity, selectivity and robustness toward practical applications in the Sb removal in natural and engineered water systems.

## 2 Carbon-based nanomaterials (CNMs)

Recently, carbonaceous sorbents have attracted considerable attention owing to their high adsorption capacity, excellent electric conductivity and rich surface chemistry (Yang et al., 2019; Duan et al., 2020). However, the main drawbacks associated with post-separation and sluggishness in kinetics greatly restricted the practical applications of traditional carbon materials (Duan et al., 2020; Cheng et al., 2021). In light of growing interests and advances of nanotechnology, CNMs are more favorable for environmental applications due to several advantages such as large surface area and outstanding mechanical strength (Wang et al., 2015a; Ganzoury et al., 2020; Gusain et al., 2020; Liu et al., 2020b).

2.1 Graphene and derivatives

Graphene is the thinnest known CNM with a single sheet of two-dimensional (2D) carbon hexagonal structure (Huang et al., 2021). As shown in Fig. 1, graphene forms the fundamental 2D building block that can be further wrapped into fullerenes (0D), rolled into carbon nanotubes (1D), and stacked into graphite (3D) (Wan et al., 2012). Both bottom-up (e.g., unzipping of CNT or rGO) and top-down (e.g., electrochemical, sonochemical exfoliation, acidic dilution of graphite) strategies are available for the synthesis of graphene (Leng et al., 2012; Huang et al., 2018). The high adsorption capacity for the removal of heavy metal ions by graphene is guaranteed by its large surface area and small thickness (Li et al., 2020a). For instance, composite graphene nanosheet/δ-MnO_2, synthesized using microwave irradiation, has been demonstrated for removing lead ions in wastewater (Ren et al., 2012). The mechanism for lead ions uptake is associated with the presence of hydroxyl and carboxyl groups on the edge of graphene and MnO_2. These groups couple with lead ions to form a tetradentate surface complex.

Graphene oxide (GO) is a graphene derivative with a large theoretical surface area (~2630 m^2/g) (Yang et al., 2015). It has abundant oxygen-containing functional groups including hydroxyl, carboxyl and epoxy groups. Hence the graphene-like layers are highly hydrophilic. The rich chemistry on GO surfaces offers high-density active sites for the adsorption of various heavy metal ions. For instance, Wang et al. (2015a) found that the GO had the Pb (II) adsorption capacity as high as 470.3 mg/g at 293 K from the pre-concentrated Pb(II) in an aqueous solution.

Reduced graphene oxide (rGO) can be easily prepared by the reduction of GO with chemical reducing agents, including hydrazine, hydroquinone, sodium borohydride
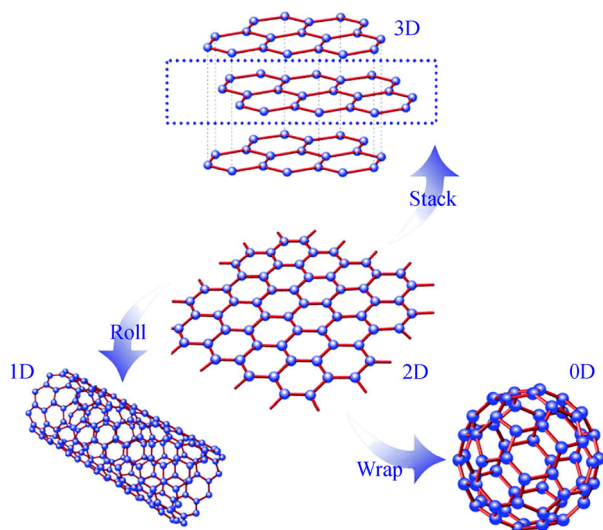
Fig. 1 Graphene is the basic building block for other carbon allotropes (Reprint from Wan et al. (2012) with permission of American Chemical Society).

and ascorbic acid, et al., by thermal treatment, or electrochemical reduction (Zou et al., 2021). The rGO and its composites have been reported capable of effectively removing heavy metal ions (Zou et al., 2016; Jiang et al., 2020). For example, Yap et al. (2020) prepared a polyamine-functionalized rGO adsorbent for the fast removing of Hg(II) from water with a high adsorption capacity of 63.8 mg/g.

In addition to the use powder form of graphene, the laminar GO membranes are the prospective candidates for nanofiltration with ultrahigh permeability, good mechanical properties, and tunable inter-layer spacing (Yu et al., 2020). However, the GO membranes may suffer from poor stability due to high hydrophilicity. Hence the GO composite membranes fabricated by immobilizing GO flakes within a polymeric matrix have been developed for water purification (Maheshkumar et al., 2014). Shukla et al. (2018) reported nanofiltration with a membrane consisting of carboxylated GO in polyphenylsulfone matrix. The polyphenylsulfone was specifically selected due to its good chemical resistance and high-temperature stability in addition to the excellent hydrolytic stability. The carboxylated GO played a role as the nanoscale additive by improving the surface charge for the removal of heavy metal ions. The resulting nanofiltration performance was demonstrated by the removal of toxic metal ions, including arsenic, chromium, cadmium, lead, and zinc with the maximum removal efficiencies of 98% and 80% for the anions and cations, respectively.

2.2 Carbon nanotubes (CNT)

One or a few layers of graphene can be rolled into single-walled or multi-walled CNT (Sarkar et al., 2018).

Although the contact surface of a single-walled CNT is much larger than that of a multi-walled CNT, the single-walled CNT is rarely used due to the high cost and difficulty in preparation. The CNT have a large specific surface area (30−500 m^2/g) and excellent electric conductivity (10^4−10^6 S/m), which have been shown capable of adsorbing pollutants via hydrophobic interactions and π-π interactions (Krishna Kumar et al., 2015). It is worth noting that the pristine CNT is not preferred because the surface hydrophobicity makes it difficult to be dispersed in an aqueous solution. Hence, surface wettability and the associated dispersibility need to be improved by chemical modifications. It is common practice to functionalize the CNT by doping oxygen, nitrogen, and sulfur heteroatoms onto the surface of CNT via oxidation, nitrogenation, and sulfuration. Figure 2 shows the schematic illustration of the techniques for the modification of CNT, which indicates the chemical agents used for the corresponding functional groups. Several studies have provided evidence that the surface functioning on CNMs could effectively increase the capacity of heavy metal adsorption (Mishra and Sankararamakrishnan, 2018; Yang et al., 2019). Mobasherpour et al. (2012) synthesized the HNO_3-treated CNT, which successfully removed Ni(II) from aqueous solutions. The oxygen functional groups introduced by the HNO_3 oxidation increased the surface density of negative charges. This in turn increased the cation-exchange capacity since the oxygen atoms on the CNT surfaces donated electrons to the adsorbed metal cations, which strengthens the coupling between the metal and the CNT.

Since the powdered CNT are prone to agglomeration, additional procedures are needed for post-dispersion. On the other hand, the CNT-based membranes became a more attractive alternative for water purification. Interweaved nanoporous CNT membranes can be fabricated by combining self-assembly and simple filtration methods (Yi et al., 2019). Yang et al. (2021) developed a highly adsorptive CNT membrane obtained from the vacuum filtration of dispersed CNT powders in water. The membrane was used as the substrate to support photocatalytic FeOOH catalysts. The produced composite FeOOH/CNT membrane offered excellent self-cleaning properties via the photocatalytic Fenton reactions. To improve the durability and stability of the modified CNT membrane, the electroless welding method was used to produce silver nano-knots between the adjacent interweaving CNT. Dynamic filtration experiments suggested that the adsorption capacities of the membrane for rhodamine B and methylene blue could be as high as 181.0 mg/g and 247.0 mg/g, respectively. Thus, robust, self-cleaning, and regenerable adsorptive membranes can be obtained by developing composite CNT materials.

Furthermore, recent advances in nanotechnology pose promise of combining conventional membrane processes with electrochemistry (Li et al., 2020; Liu et al., 2020a). The electrochemical treatment of water using CNT-based
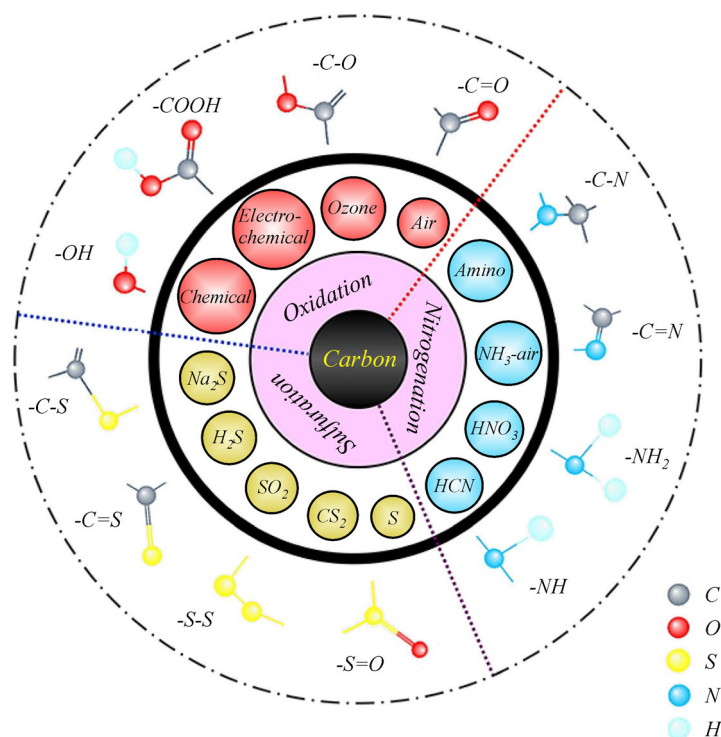
Fig. 2 Modification techniques to functionalize carbon-based nano-adsorbents with various functional groups (Reprint from Yang et al. (2019) with permission of Elsevier).

membranes enables physical adsorption followed by on-site chemical oxidation of pollutants. In addition, the mass transport of ionic compounds can also be improved by electric-field assisted migration, which can be used either as a standalone unit or in a polishing step. Liu et al. (2019a) reported an electroactive filter consisting of nanoscale polyaniline-modified CNT. With the external electric field, the highly toxic Cr(VI) was effectively converted to the less toxic Cr(III), which was further sequestered by the nanoscale polyaniline nanoparticles. The CNT-based electroactive filters may offer a new route for the highly effective removal of highly toxic metal ions.

2.3 Other CNMs

Besides the aforementioned CNMs, 1D carbon nanofibers have also attracted considerable attention toward the removal of heavy metal ions owing to their high surface-to-volume ratio and the capability to establish π-π electrostatic interactions (Luo et al., 2015; Zhou et al., 2020). The functionalization of carbon nanofibers can be achieved easily, which provides new opportunities to fabricate multi-functional CNMs. For example, Thamer et al. (2019) prepared the poly(m-phenylene diamine)-functionalized carbon nanofibers for fast removal of Pb^{2+} in water with adsorption capacity of 354.5 mg/g. Besides, 0D fullerene may also serve as a promising alternative to remove heavy metal ions due to its large specific surface

area, lower degree of aggregation and abundant defects (Kroto et al., 1985). For instance, Alekseeva et al. (2016) reported the adsorption of Cu^{2+} using fullerene with adsorption capacity of 927.1 mg/g. Overall, CNMs may offer effective and reliable options for the removal of diverse heavy metal ions from water bodies.

3 Antimony removal by carbon-based nano-materials

3.1 Adsorption

3.1.1 Graphene-based sorbents

The 2D graphene has unique advantages of large surface area and planar configuration for the adsorptive removal of heavy metal ions. Leng et al. (2012) found that Sb(III) could be absorbed by the pristine graphene with a maximum sorption capacity of 10.9 mg/g for a duration of 4 h under alkaline condition. These findings suggested the graphene to be a promising adsorbent for the removal of Sb in water. Since then, much effort had been devoted to increasing the sorption capacity with improved adsorption kinetics. One promising strategy is to integrate functional polymer materials with graphene. Saleh et al. (2017) modified graphene with polyamide via interfacial poly-merization, which showed an enhanced Sb(III) adsorption

capacity of 158.2 mg/g, a value being 15 times higher than that of the pristine graphene. More importantly, the polyamide coated graphene achieved faster sorption kinetics, reaching the adsorption equilibrium in less than 30 min. This value was much lower than that of several state-of-the-art adsorbents which took several hours or even longer reaching equilibrium (Yu et al., 2013; Guo et al., 2014). As shown in Fig. 3(a), the rapid Sb(III) adsorption on the polyamide/graphene composite could be attributed to (1) a large number of oxygen-containing functional groups and surface defects on the graphene sheets, (2) the increased monolayer surface coverage at the edge of the graphene or polyamide, and (3) the formation of monodentate, bidentate, and tridentate ligands on the polyamide chain. The advantages of the cost-effective polyamide/graphene composite material are related to the ease of regeneration with high uptake capacities, making it hold great promise for the removal of metal ions from water.

The surface oxy-functional groups play a crucial role in Sb removal, which was demonstrated by the GO with sufficient exposed surface moieties. Yang et al. (2015) reported that the GO could adsorb Sb(III) with a specific capacity of 36.5 mg/g, which is 3.3 times higher than that of the pristine graphene. They attributed this to the involvement of oxygen-containing functional groups on the GO surface. In addition, GO also showed rapid Sb

adsorption kinetics indicated by an adsorption equilibrium time of within 40 min. Similarly, Capra et al. (2018) demonstrated that the oxidized and exfoliated graphite nanoplatelets outperformed graphene with the maximum adsorption capacity of 18.2 mg/g derived from the Langmuir isotherm. The higher performance was associated with the higher density of carboxylic groups as the active adsorption sites on the surface of graphite nanoplatelets (Fig. 3(b)).

Although GO exhibited decent adsorption behavior toward heavy metal ions, its sorption selectivity and capacity could be further improved with new GO-based derivatives. GO was used as the substrate material to support organic and inorganic modifiers with maintained large surface area and excellent mechanical stability. Meanwhile, the adsorption capacity for Sb can also be improved by controlled incorporating of other active components. Dong et al. (2015) prepared GO/schwert-mannite composite sorbent for the Sb(V) removal. The adsorption capacity of 158.6 mg/g was achieved which is superior to either GO or schwertmannite alone, indicating effectiveness of both schwertmannite and GO for Sb(V) removal. The synergistic effect between GO and schwert-mannite could be originated from the interactions of Sb(V) with Fe-O surface sites on schwertmannite and the surface functions on GO (e.g., carboxyl, anhydride and phenol groups). On the other hand, the high dispersible of GO in
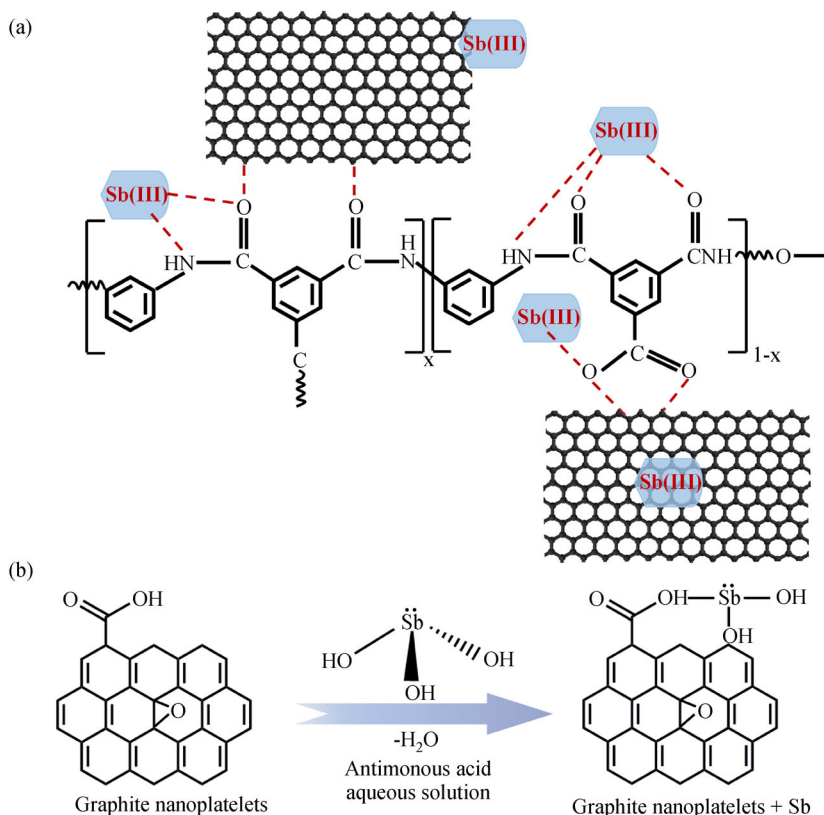
Fig. 3 (a) Proposed mechanisms for the adsorption of Sb(III) onto polyamide/graphene. (Adapted from Saleh et al. (2017)). (b) Proposed mechanism for adsorption of Sb (III) on graphite nanoplatelets (Adapted from Capra et al. (2018)).

water may make it difficult to be separated from the aqueous solution. To address this issue, super-paramagnetic composite nanomaterials were developed allowing efficient post-separation of CNMs from water. Yang et al. (2017) synthesized a magnetic Fe_3O_4/GO composite that accomplished 95% removal of Sb(III) with rapid solid-liquid separation by the external magnetic field. The magnetic composite nanomaterials represent a new way with highly efficient separation of the used nano-adsorbents.

Owing to several interesting physical and chemical properties, rGO has also attracted an extensive interest for its application in the removal of Sb. Zou et al. (2016) fabricated a 3D nanostructured composite of rGO/Mn_3O_4 adsorbents using a facile method of reflux-condensation followed by solvothermal reactions. Such a peculiar 3D structure exhibited several intriguing properties compared with the conventional members of the carbon material family. One prominent advantage of rGO is its ability to effectively prevent the agglomeration of Mn_3O_4 nanoparticles. Based on the Langmuir isotherms, the theoretical maximum adsorption capacities of Sb(III) and Sb(V) on rGO/Mn_3O_4 were estimated to be 151.8 mg/g and 105.5 mg/g, respectively. Both values are much higher than the majority of those reported adsorbents for the Sb removal (Navarro and Alguacil, 2002; Yu et al., 2014). On the other hand, the core-shell microspheres of functionalized CNMs have also been the focus of new development. Several methods have been developed to fabricate such core-shell architectures, including template-directed formation, chemical deposition, colloidal aggregation, laser-induced assembly and self-assembly (Yoo et al., 2009; Lee et al., 2012). However, the process normally requires the use of delicate, expansive templates with cumbersome post-treatment processes. To address these challenges, Jiang et al. (2020) proposed a template-free, self-assembly technique to synthesize actiniaria-like core-shell Co_3O_4/rGO nanocomposite materials. The strong interactions between the rGO and the cobalt oxide were essential for the formation of the actiniaria-like core-shell structure of the Co_3O_4/rGO. The oxygen involved in both Co_3O_4 (O-Co) and rGO (H-O-C) took part in the adsorption of Sb(III). The Co_3O_4/rGO nanocomposite exhibited a high anti-interference performance with the maximum Sb(III) adsorption capacity of 151.0 mg/g. A similar synthesis strategy could also be used for the production of other core-shell structured nanomaterials. These examples illustrate the potential of graphene-based nanomaterials for the low-cost, highly efficient, and environmentally benign absorption of Sb in water.

3.1.2   CNT-based sorbents

CNT-based 1D sorbents are another class of promising CNMs, which have also been examined for the Sb removal application. Table 1 summarized several selected reports on the removal of Sb using CNT and their derivatives. According to Salam and Mohamed (2013), the removal of Sb(III) by CNT proceeded in several steps, involving (1) the diffusion of metal ions through the liquid layer arriving surface of CNT, (2) the adsorption of Sb(III) ions on the CNT surface, and (3) the intra-particle diffusion and adsorption of metal ions between the CNT aggregates. It is worth noting that the CNT demonstrated a very limited adsorption capacity of 0.3 mg/g at pH 7.0 and 298 K. This value is much lower than that of other CNMs such as graphene (10.9 mg/g). Besides that, the CNT were also subject to poor selectivity for the removal of Sb. Attempts had been made to improve both adsorption capacity and selectivity of CNT by tailoring the surface chemistry. For example, partially oxidized CNT were capable of efficiently adsorbing heavy metal ions through electrostatic attraction and the formation of chemical bonds. Mishra and Sankararamakrishnan (2018) produced iodide-grafted CNT and thiol-functionalized CNT by oxidation. Results indicated that the adsorption capacities for Sb(III) of this iodide- and thiol-functionalized CNT were increased to 166.6 mg/g and 125.0 mg/g, respectively. Compared with pristine CNT, the higher adsorption capacities of modified adsorbents could be attributed to strong bonding interaction between the Sb(III) and the functional groups associated with iodide and thiol ligands. In addition, the contact time of 3.0 h was sufficient for the adsorption of Sb(III) using iodide-functionalized CNT, whereas only 2.5 h was required to reach Sb(III) adsorption equilibrium when thiol-functionalized CNT was used. The detailed Sb(III) adsorption mechanism was further evidenced by the formation of antimony iodide and sulfide complexes. Moreover, the functionalized CNT is stable over a wide range of pH, which is important for the flexibility of its applications.

CNT loaded with specific metal or metal oxides nanocrystals could also be an effective strategy to improve the Sb adsorption performance. Mishra et al. (2016) synthesized nanoscale zero-valent iron-functionalized CNT (nZVI/CNT) used for the removal of Sb(III) with the adsorption capacity of 250.0 mg/g, which is approximately three orders of magnitude greater than that by the pristine CNT (0.4 mg/g). The dramatic increase in the adsorption capacity is correlated to the formation of Fe-O bonds when adsorbing Sb(III) through a two-steps process. In details, the Sb(III) species was first adsorbed on the surface of nZVI/CNT, followed by the complexation with Fe(II) or Fe(III) to form mixed hydroxides. The kinetics for Sb(III) uptake by nZVI/CNT were rapid initially and nearly 50% of Sb(III) was adsorbed within the first 60 min. The stability of the sorbent at different pH and temperature conditions is an important factor in practical application. Yu et al. (2013) prepared a novel CNT modified with iron oxide (Fe_2O_3/CNT) by the co-precipitation method. The prepared Fe_2O_3/CNT material showed the minor influence of the solution pH and working temperature on the removal

Table 1 Applications of carbon-based nanomaterials for the removal of antimony.

No.	Adsorbents	Sorption capacities (mg/g)			pH	T (°C)	Initial Concentration (mg/L)	BET surface area (m²/g)	Adsorption isotherm	Kinetics model	References
		Sb(III)	Sb(V)	Sb(total)							
1	Graphene	10.9	–	–	11.0	30	1–10	154.4	Langmuir	second-order	Leng et al., 2012
2	Polyamide/Graphene	158.2	–	–	5.0	20	1–25	421	Langmuir	second-order	Saleh et al., 2017
3	GO	36.5	–	–	7.0	25	0–30	315.6	Langmuir	first-order	Yang et al., 2015
4	Graphite Nanoplatelets	18.2	–	–	7.0	20	0–1	205	Langmuir	second-order	Capra et al., 2018
5	GO/Schwertmannite	–	158.6	–	7.0	25	0–60	287.6	Langmuir	second-order	Dong et al., 2015
6	Fe₃O₄/GO	9.6	–	–	7.0	25	0–500	–	Langmuir	first-order	Yang et al., 2017
7	rGO/Mn₃O₄	151.8	105.5	–	6.8	20	10–1000	44	Langmuir	second-order	Zou et al., 2016
8	Co₃O₄/rGO	151.0	165.5	–	–	25	0–280	53.6	Langmuir	second-order	Jiang et al, 2020
9	CNT	0.3	–	–	7.0	25	4	89.2	Langmuir	second-order	Salam & Mohamed, 2013
10	Iodide-functionalized CNT	200.0	–	–	7.0	25	10–100	105.8	Langmuir	second-order	Mishra & Sankararamakrishnan, 2018
11	Thiol-functionalized CNT	140.9	–	–	7.0	25	10–100	111.9	Langmuir	second-order	Mishra & Sankararamakrishnan, 2018
12	nZVI/CNT	250.0	–	–	5.0	25	0–200	132	Langmuir	second-order	Mishra et al., 2016
13	Fe₂O₃/CNT	6.2	–	–	7.0	25	0–3.2	96.9	Freundlich	first-order	Yu et al., 2013
14	Biochar	85%	68%	–	5.0	25	0.5–5.0	20.2	Langmuir	–	Vithanage et al., 2015
15	Ce-doped magnetic biochar	–	25.0	–	7.5	25	10–100	230.7	Langmuir	second-order	Wang et al., 2019
16	MnFe₂O₄/biochar	237.5	–	–	7.0	25	25–500	30.4	Langmuir	second-order	Wang et al., 2018c
17	La-doped magnetic biochar	–	18.9	–	7.0	25	10–100	287.1	Langmuir	second-order	Wang et al., 2018b
18	Fe₃O₄/Fe₂O₃/carbon nanosphere	234.3	–	–	5.0	20	100–1000	192.6	Langmuir	second-order	Ren et al., 2020
19	Fe₂O₃/carbon nanosphere	102.8	–	–	5.0	20	10–200	134.9	Langmuir	second-order	Ren et al., 2020
20	Iron oxides/carbon nanosphere	233.6	–	–	6.0	20	50–1000	88.3	Langmuir	second-order	Wang et al., 2018a
21	FeCl₃/activated carbon	2.6	–	–	7	25	0.5–3.5	940.0	Langmuir	first-order	Yu et al., 2014
22	ZrO₂-carbon nanofiber	70.8	57.2	–	7	25	10–500	106.3	Langmuir	second-order	Luo et al., 2015
23	TiO₂-CNT (filter)	–	–	95	7	25	0–12	178	Langmuir	second-order	Liu et al., 2019c
24	Titanate-CNT (filter)	–	–	82.4	7	25	0–5	128.6	Langmuir	second-order	Liu et al., 2019b
25	MIL-88B(Fe)-CNT (filter)	–	–	13.1	7	25	1	382.3	Langmuir	first-order	Li et al., 2020
26	Goethite/CNT (filter)	–	–	63.5	7	25	0–5	98.1	Langmuir	first-order	Hu et al., 2021

of Sb(III), which is an advantage for industrial water purification.

3.1.3   Other carbon-based sorbents

Besides the CNT- and graphene-based carbon nanomaterials, other carbon materials were also evaluated for the elimination of Sb. For instance, biochar is an emerging and low-cost carbon-rich sorbent produced from agricultural residues, wood, and wasted feedstock under oxygen-free or oxygen-deficient conditions (Su et al., 2021). However, few papers reported the mechanistic insight into the interaction between biochar and trace elements (e.g., Sb and As). Vithanage et al. (2015) demonstrated that the biochar from soybean stover produced by at low-temperature pyrolysis (300°C) could strongly bind Sb(III) and Sb(V). Nevertheless, the negatively charged surface of pristine biochar limited its ability to adsorb anionic Sb. Hence, several methods have been developed to modify the biochar to improve the Sb adsorption. Wang et al. (2019) synthesized a Ce-doped magnetic biochar for efficient Sb(V) adsorption. The modified biochar exhibited a high adsorption capacity of 25.0 mg/g, which is one order of magnitude higher than that of the un-modified biochar. From the adsorption measurements and the physicochemical analyses, the driving force for the Sb(V) adsorption on the Ce-doped magnetic biochar is associated with the surface complexation, hydrogen bonding, electrostatic attraction and ligand exchange, shown in Fig. 4, within which, the formation of Ce-O-Sb complex and the ligand exchange was identified as the key mechanism for the Sb(V) adsorption. Similarly, a jacobsite-biochar nanocomposite ($MnFe_2O_4$-biochar) was also produced, using a co-precipitation method, for the simultaneous removal of Sb(III) and Cd(II) from water (Wang et al., 2018c). The maximum adsorption capacities of 237.5 mg/g were obtained for Sb(III). XPS spectra of Sb(III)-adsorbed $MnFe_2O_4$/biochar confirmed the presence of Sb(V). This confirmed that the chemical bonding was responsible for the Sb(III) adsorption, which in turn explained why the modification with $MnFe_2O_4$ is important for the improved metal ion adsorption by biochar. Ren et al. (2019) reported the facile hydrothermal and co-precipitation method to synthesize two types of magnetic adsorbents for the efficient removal of Sb(III) in water, namely Fe_3O_4/Fe_2O_3/carbon nanospheres and Fe_2O_3/carbon nanospheres. From the Langmuir isotherms, the theoretical maximum adsorption capacity of Sb(III) was as high as 283.3 mg/g and 117.4 mg/g by these two nanosphere samples, respectively. Besides, the composites also demonstrated high removal rates for low-concentration Sb(III). In a similar study, Wang et al. (2018a) developed mesoporous carbon nanospheres composited with active Fe_2O_3 particles. The incomplete carbonization of the carbon sphere allows the formation of developed porous structure acting as microchannels for the encapsulation of active iron oxides. The theoretical maximum Sb(III) adsorption capacity was as high as 233.6 mg/g benefited from the honeycomblike structure decorated with Fe_2O_3 nanoparticles inside the microchannels. Luo et al. (2015) demonstrated an electrospinning method for the synthesis of zirconium oxide (ZrO_2) modified carbon nanofibers (ZCN) for the removal of both Sb(III) and Sb(V). Under the pH-neutral condition, the ZCN showed faster adsorption kinetics in the first 30 min, while the adsorption equilibrium was reached within 50 min with 70.8 mg/g and 57.2 mg/g of the maximum adsorption capacities for Sb(III) and Sb(V), respectively, shown in Figs. 5(a) and 5(b). The formation of an ionic bond of Sb(III)/Sb(V) on the surfaces of t- and m-ZrO_2 (111) is evident in Fig. 5(c), indicating the vital role of the Zr-O sites for the Sb sequestration. The above examples suggest an increased number of carbon-based nano-adsorbents were developed for the efficient removal of Sb from water.
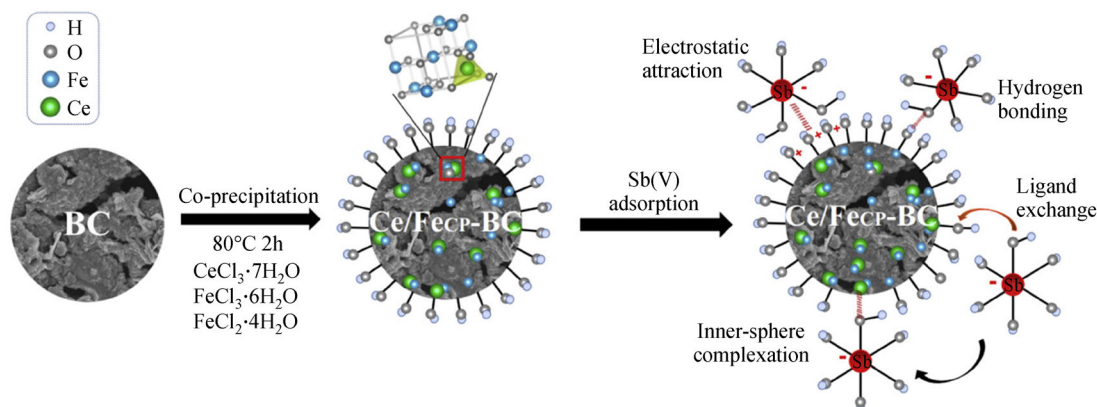
Fig. 4   Schematic diagram of the formation of Ce-doped magnetic biochar and its mechanisms for Sb(V) adsorption. Adapted from Wang et al. (2019).
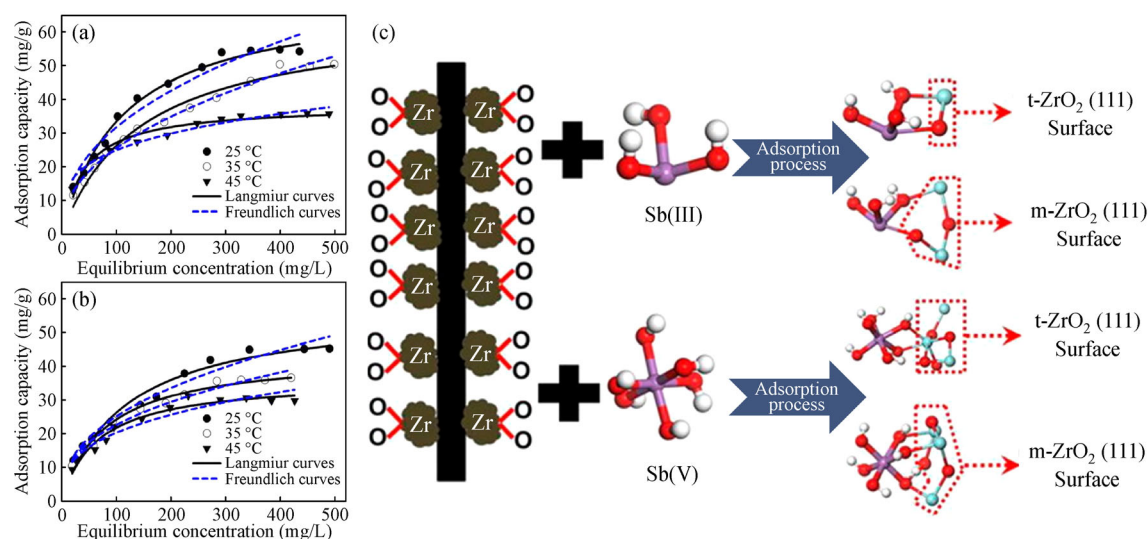
Fig. 5 Adsorption isotherm with different temperatures for (a) Sb(III) and (b) Sb(V) on ZCN. (c) Proposed mechanisms for the adsorption of Sb(III)/Sb(V) onto ZCN. Adapted from Luo et al. (2015).

3.2 Membrane separation

The powdered CNMs may be faced with inherent drawbacks such as agglomeration and difficulty in post-separation. Alternatively, the membrane design could be a better option to alleviate these challenges. In addition, the membrane can also incorporate functional nanoparticles to form mixed matrix membranes (MMMs) or to synthesize the carbon-based membranes directly. Such hybrid materials have the synergistic advantages of both nanoparticles (high selectivity and high surface area) and the polymeric matrix (porous structure and high water flux) (Nasir et al., 2019). Notably, the free-standing membrane containing CNMs, including 1D CNT and 2D graphene, can be fabricated by the simple and facile vacuum-filtration method. Unlike powered materials, which require separation and recovery, these carbon membranes can act as stand-alone units for the removal of heavy metals without the need for expansive post-separation.

3.2.1 Graphene-based membranes

GO represents a promising carbon membrane material with abundant oxygen-containing functional groups (e.g., hydroxyl and carboxyl) at the edges of the laminar nanosheet. The surface hydrophilicity is important for providing excellent permeation of water molecules through the membrane matrix. However, compared with extensive investigation on the removal of As, only a few literatures were reported on the Sb removal. Sb has relatively larger ionic diameter (1.41×10^{-10} m vs. 1.21×10^{-10} m) and slower mobility in solution than As (Guo et al., 2021). As and Sb display the same range of oxidation states in aquatic environment. Both occur as oxyanions, primarily in the tri-(III) or pentavalent (V) state and are often considered to

behave similarly (Wilson et al., 2010). Cetinkaya et al. (2018) used the air-spray method to prepare the GO-coated microfiltration membranes offering 98% As removal under 5 bar of applied pressure. Pal et al. (2018) also reported 98% As removal achieved from the GO-incorporated polyethersulfone membrane. It is worth noting that the selection of functional nanomaterial adsorbent is crucial for the adsorptive performance of the MMMs for heavy metal removal. Shahrin et al. (2019) developed new adsorptive MMMs with improved performance by incorporating the highly adsorptive GO-manganese ferrite nanomaterial into the polyethersulfone membrane. The GO-manganese ferrite nanomaterial was synthesized via a chemical co-precipitation method. The GO-manganese ferrite-incorporated MMMs were fabricated using a non-solvent induced-phase inversion method. The optimal adsorption performance was achieved with a maximum adsorption capacity of 75.5 mg/g for the As removal at pH = 4.0. It is reasonable to infer that similar adsorption mechanism and performance could also be expected for the Sb removal.

3.2.2 CNT-based membranes

The metal oxide-modified CNT offered significant potential as a highly effective adsorbent for the abatement of Sb in water. However, the adsorptive kinetics of powdered nanomaterials remains low, which hinders its practical applications. Furthermore, the speciation of Sb in an aqueous solution was strongly correlated with its physico-chemical properties. The most abundant species of Sb exist mainly in the form of inorganic Sb(III) and Sb(V). However, the Sb(III) is 10 times more toxic than the Sb(V). Compared with the negatively-charged Sb(V), the removal of aqueous Sb(III) is challenging due to the

charge-neutral state (i.e., Sb(OH)$_3$) over a broad pH range (e.g., pH 3-9) (Luo et al., 2015). To mitigate this problem, Sb(III) need to be oxidized to Sb(V) before being removed by the adsorption. However, such a "two-step" approach will inevitably increase the complexity of the system with additional consumption of chemicals. Hence, it is highly desirable to exploit the "one-step" process for the detoxification and adsorption of Sb(III).

With high surface area and excellent electric conductivity, the CNT can be easily fabricated into a free-standing electroactive membrane. Using an external electric field, it is feasible to realize the oxidation and sequestration of Sb(III) simultaneously. Our group has provided a proof-of-concept demonstration of a rationally designed, dual-functional electrochemical filtration system for the decontamination of Sb(III). The system consists of a CNT membrane anode functionalized with TiO$_2$ nanoparticles, accompanied by a perforated Ti foil cathode (Liu et al., 2019c). Such an innovative design integrates the advantages of membrane filtration with electrochemical redox power. As shown in Fig. 6(a), upon application of an external electric field (e.g., 2 V), the highly toxic Sb(III) was oxidized into the less-toxic Sb(V). Subsequently, the Sb(V) was sequestered by the adsorption on the TiO$_2$ nanoparticles (10 nm). Higher than 95% of Sb(III) was successfully removed over the time of 8 h under the continuous filtration condition. The residual Sb in water was in the less toxic form of Sb(V), indicating the completion of oxidation of Sb(III) during the filtration process. Moreover, both the sorption kinetics and capacity were increased with the applied voltage (Fig. 6(b)). For example, by increasing the voltage from 0 V to 2 V, the maximum Sb removal capacity was increased from 3.3 mg/g to 4.2 mg/g, accompanied by a decreased time from >8 h to 3 h to reach the equilibrium. Meanwhile, the Sb(III) sorption capacity has negligible changes with the pH in the range of 5–9 (Fig. 6(c)). More importantly, the Sb(III) removal performance could be further enhanced by replacing TiO$_2$ with other Sb-specific nanomaterials, such as titanate nanowires, goethite, and nZVI (Liu et al., 2019b; Hu et al., 2021). Alternatively, the CNT membrane cathode could also catalyze the selective two-electron reduction of O$_2$ to produce H$_2$O$_2$. This process activates the O$_2$ to create the electro-Fenton conditions for the detoxification of Sb(III). Li et al. (2020b) designed a flow-through electrochemical system consisting of the iron oxychloride (FeOCl)-functionalized CNT membrane as the cathode with a perforated Ti anode. With an appropriate cathode potential, the electro-produced H$_2$O$_2$ could be efficiently decomposed to HO•, leading to an ultra-fast detoxification of Sb(III) with just a single pass through the filtration system ($\tau < 3$ s). These observations are of great value for gaining the understanding and optimization of the Sb(III)/E-Fenton system, which provides a green and robust nanotechnology for the efficient Sb(III) decontamination in an aqueous solution.
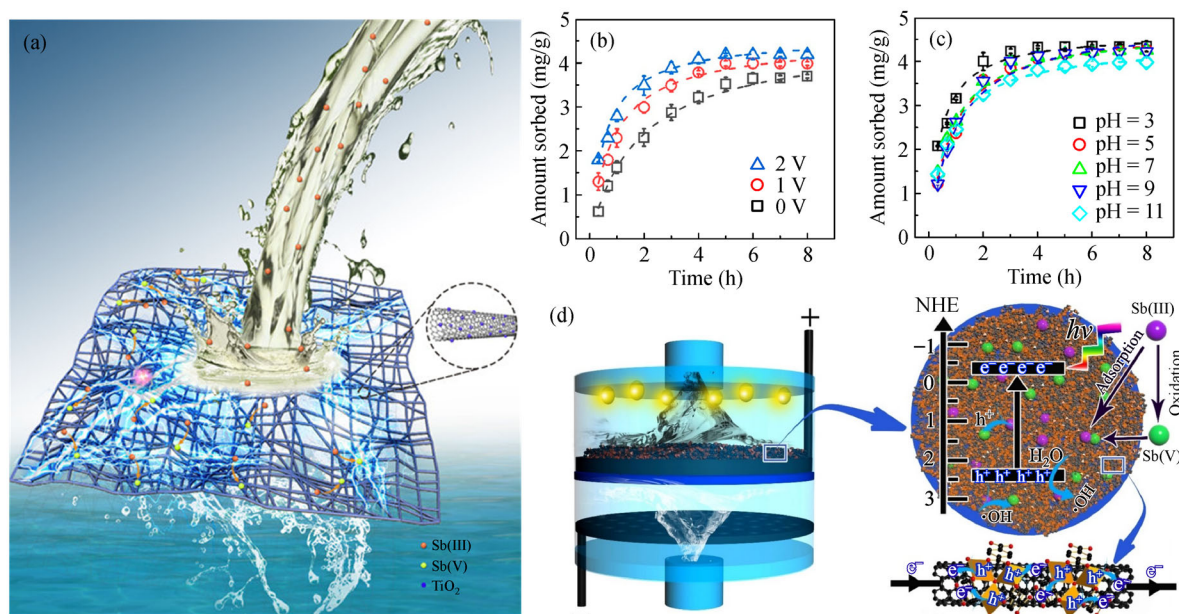
Fig. 6 (a) Schematic illustration of the proposed working mechanism toward Sb(III) removal using the electrochemical filtration system (Reprint from Liu et al. (2019c) with permission of American Chemical Society). Effect of (b) applied voltage (0-2 V) and (c) pH (3-11) on Sb (III) sorption (Reprint from Liu et al. (2019c) with permission of American Chemical Society). (d) Schematic illustration of the plausible photoelectrochemical decontamination mechanism of Sb(III) (Reprint from Li et al. (2020) with permission of Elsevier).

The system efficacy can be further enhanced by the incorporating of photo-responsive nanoparticles. For example, Li et al. (2020) developed a photoelectrochemical membrane by integrating the photoactive Fe-based MOF (e.g., MIL-88B(Fe)) with CNT. In this system, the CNT serves as a conductive scaffold to host nanoscale MIL-88B(Fe) and to conduct photogenerated electrons. The plausible mechanism of Sb(III) removal is illustrated in Fig. 6(d). In details, the Sb(III) could be first oxidized to the low-toxicity Sb(V) during the photoelectrochemical process. The resulting Sb(V) could be effectively sequestered by the loaded Fe-MOFs. Results showed that the optimal performance of 97.7±1.5% Sb(III) conversion with 92.9±2.3% Sb_{total} removal could be achieved by a single pass filtration ($\tau < 2$ s). Therefore, the CNT-based membrane could provide an affordable alternative for the removal of Sb(III) from water with promised efficacy.

4 Prospects and conclusions

4.1 Functionalization with affordable functional nanomaterials

The successful enhancement in the adsorption performance of modified CNMs prompts the search for environmentally friendly, biodegradable, and cost-effective natural compounds, such as amino acids (e.g., *L*-cysteine) and sugars (e.g., chitosan) for the modification of CNMs (Tripathy et al., 2020; Zeng et al., 2020a; Vakili et al., 2021). For instance, *L*-cysteine can strongly coordinate with various toxic metal ion pollutants via the interaction with the functional groups, such as $-COOH$, $-SH$, and $-NH_2$. White et al. (2009) demonstrated that the poly-*L*-cysteine coated magnetic-Fe_2O_3 nanoparticles had higher metal ion adsorption capacities than that of the uncoated nanoparticles. In addition, sugars, such as chitosan, are also effective for the removal of toxic pollutants due to the abundant hydroxyl groups. Although they are chemically stable, they normally have high reactivity with good selectivity by forming specific chelation. According to Croitoru et al. (2020), the GO powders could be well dispersed in the chitosan solution, involving a large number of hydrogen bonding between the chitosan and GO. Moreover, chitosan could synergistically adsorb Sb(III) by both chelating and electrostatic attractions (Zeng et al., 2020b). Thus, it is feasible to develop CNMs functionalized with natural compounds to enhance the removal capacity of Sb.

4.2 Functionalization with magnetic composites

The post-separation of exhausted CNMs from an aqueous solution remains a challenge. Compared with centrifugation and filtration, magnetic separation is much more favorable for the separation of adsorbents from aqueous solutions. Several adsorbent materials (e.g., Fe_3O_4 and nZVI) are paramagnetic and can respond to the external magnetic field. Thereby, the separation can be easily achieved under the action of an external magnetic field (Li et al., 2012; Dong et al., 2019). However, their specific adsorption affinity toward Sb has yet to be satisfied. Thus, growing interests have been focused on the doping of transition metals into the magnetite spinel structure to improve the adsorption of Sb. Creating surface defects, introducing functional groups, increasing the surface charge and adjusting the electronic properties can greatly optimize the adsorption performance of CNMs. For instance, a Fe-Zr bimetal oxide was fabricated via the co-precipitation method. It exhibited a significant enhancement in the Sb(V) removal with respect to the ferric oxide (Li et al., 2012). Likewise, Zhu et al. (2017) introduced Ce dopant into the Fe_3O_4 lattice, which resulted in more than 5 times of improvement in the Sb(V) adsorption capacity, compared with pure Fe_3O_4, due to the increased number of surface hydroxyl groups. Dimpe et al. (2017) synthesized the composites of activated carbon that was coated with a mixture of iron oxide and manganese oxide nanoparticles by a sol-gel method. The composite combined the benefits of the oxidation power of MnO_2 with the adsorption ability of Fe_2O_3 and active carbon, together with the magnetic property of Fe_2O_3. In another work, La-doped magnetic biochar was fabricated via a co-precipitation method. It exhibited improved physicochemical characteristics with excellent Sb(V) adsorption performance. The pristine biochar and the un-doped magnetic biochar had the Sb(V) adsorption capacities of 2.2 mg/g and 4.9 mg/g. However, this value was greatly increased to 18.9 mg/g for the La-doped magnetic biochar at the pH-neutral condition. Hence, the modification of CNMs with bimetallic composite may offer a low-cost and easy-to-handle route for the removal of Sb contamination from water.

4.3 Development of regeneration strategies

Regeneration is an essential metric to evaluate the economic value of an adsorbent. Although the CNMs show great potential in the removal of both organic and inorganic contaminants, their industrial applications are ultimately hindered by their high cost with negative environmental implications. Hence, effective methods for recycling or regenerating the CNMs need to be developed. Conventional regeneration strategies for heavy metal-saturated CNMs include chemical desorption using strong acids, bases, or organic solvents to enable their reuse in successive cycles. For example, the Sb-saturated oxidized CNT coated with nZVI could be regenerated by an acid wash with 0.05 mol/L HCl (Mishra et al., 2016). The recovery of Sb(III) saturated GO was significantly improved when 0.1 mol/L of EDTA solution was added in the washing solution (Yang et al., 2015).

Despite these effective regeneration methods, some

inherent drawbacks remain, including the consumption of large quantities of chemicals and the generation of secondary contamination. A true environment-friendly and efficient procedure is strongly required with the desorption of concentrated pollutant based on physical conditions without the need for chemicals (e.g., light, sound, electric field, and magnetic field). Currently, regeneration methods based on electrochemistry showed a promise of application prospects. In such a case, the sorption capacity depends on the surface charge of the adsorbents that can be regulated by electrochemistry (Pan et al., 2018). Ganzoury et al. (2020) demonstrated the adsorption of copper by carboxylic acid-functionalized CNT and realized the regeneration by applying an electric field. As shown in Fig. 7, with the application of external electric potential, the CNT membrane electrode was performing the regeneration process. The percentage of Cu desorbed from the CNT membrane increased with the increase of the applied potential from 1 to 3 V (vs. Ag/AgCl). It could be assumed that the number of free positive charge on the anode surface was determined by the positive potential, which facilitated the electrostatic repulsion between the CNT and the adsorbed Cu^{2+} ions.

4.4 Fabrication of CNMs from biomass

Eco-friendly and cost-effective procedures for mass production of CNMs are urgently needed for larger-scale application to remove Sb in water. To this end, the naturally abundant biomass can be supplied as green and sustainable carbon-rich biomass for mass production of CNMs. One typical example is the glucose selected as feed stock for preparation of graphene because glucose is the most abundant carbonaceous material and intermediates in nature (Khan et al., 2021). Zhang et al. (2014) reported the preparation of graphene using glucose as raw material in the presence of $FeCl_3$ serving as template and catalyst. The resulting electric conductivity of the few-layered graphene sheets was comparable to that synthesized by chemical vapor deposition. Wang et al. (2015b) developed a scalable method to prepare carbon spheres using hemp stem, and the final product possesses a large surface area up to 3062

m^2/g due to abundant micropores and oxygen-containing functional groups.

4.5 Environmental impacts of CNMs

Despite several advantages of the CNMs, the potential environmental impacts may be also the issue of importance in practical applications. However, there has been very limited effort devoted to relevant studies, especially the adverse environmental impact of pristine CNMs and the CNMs adsorbed with highly toxic Sb during production, utilization and post treatment. Das et al. (2018) reported potential toxic effects of CNT due to their high reactivity with various biomolecules present in water system. In addition, some CNMs (e.g., multiple-walled CNT) are carcinogenic to mesothelial cells, and their pathogenic mechanism resembles that of asbestos (Madannejad et al., 2019). The carcinogenicity of these materials is dependent on several complex factors such as the length, rigidity, diameter and surface modification of CNTs (Zhao and Deng, 2015). Therefore, particular emphasis needs to be placed on developing reliable manners (e.g., life cycle assessment) so as to more objectively access the environmental impact of CNMs in the context of overall lifetime from cradle to grave in future.

4.6 Conclusions

Currently, the removal of Sb from aqueous solutions is of particular interest and concerns. Different types of CNMs reviewed here possess unique properties that can be exploited for the Sb removal from water. Numerous advanced functional CNMs have offered superior adsorption performance for the removal of Sb. Adsorption capacity and selectivity of these nanomaterials are usually enhanced by modifying their surfaces with appropriate functional groups. Overall, adsorptive removal of low-level Sb by CNMs may provide great potential to be further optimized for various applications. The nano-sized materials behave differently from their bulk counterparts, and the environmental impacts of CNMs remain unexplored, which deserves further investigation in future.
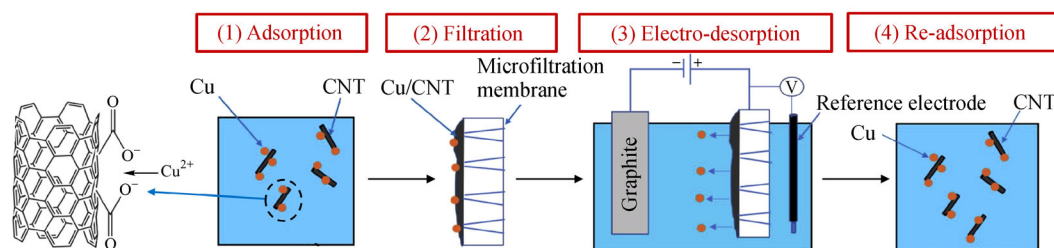
Fig. 7 Schematic approach for Cu adsorption-electrodesorption process on CNT (Adapted from Ganzoury et al. (2020)).

References

Alekseeva O V, Bagrovskaya N A, Noskov A V (2016). Sorption of heavy metal ions by fullerene and polystyrene/fullerene film compositions. Protection of Metals and Physical Chemistry of Surfaces, 52(3): 443–447

Boreiko C J, Rossman T G (2020). Antimony and its compounds: Health impacts related to pulmonary toxicity, cancer, and genotoxicity. Toxicology and Applied Pharmacology, 403: 115156

Capra L, Manolache M, Ion I, Stoica R, Stinga G, Doncea S M, Alexandrescu E, Somoghi R, Calin M R, Radulescu I, Ivan G R, Deaconu M, Ion A C (2018). Adsorption of Sb (III) on oxidized exfoliated graphite nanoplatelets. Nanomaterials (Basel), 8(12): 992

Cetinkaya A Y (2018). Performance and mechanism of direct As(III) removal from aqueous solution using low-pressure graphene oxide-coated membrane. Chemical Papers, 72(9): 2363–2373

Chen A S C, Wang L, Sorg T J, Lytle D A (2020). Removing arsenic and co-occurring contaminants from drinking water by full-scale ion exchange and point-of-use/point-of-entry reverse osmosis systems. Water Research, 172: 115455

Cheng N, Wang B, Wu P, Lee X, Xing Y, Chen M, Gao B (2021). Adsorption of emerging contaminants from water and wastewater by modified biochar: A review. Environmental pollution (Barking, Essex: 1987), 273: 116448

Croitoru A M, Ficai A, Ficai D, Trusca R, Dolete G, Andronescu E, Turculet S C (2020). Chitosan/graphene oxide nanocomposite membranes as adsorbents with applications in water purification. Materials (Basel), 13(7): 1687

Das R, Leo B F, Murphy F (2018). The toxic truth about carbon nanotubes in water purification: a perspective view. Nanoscale Research Letters, 13(1): 183

Deng S B, Bei Y, Lu X Y, Du Z W, Wang B, Wang Y J, Huang J, Yu G (2015). Effect of co-existing organic compounds on adsorption of perfluorinated compounds onto carbon nanotubes. Frontiers of Environmental Science & Engineering, 9(5): 784–792

Dimpe K M, Nyaba L, Magoda C, Ngila J C, Nomngongo P N (2017). Synthesis, modification, characterization and application of AC@Fe$_2$O$_3$@MnO$_2$ composite for ultrasound assisted dispersive solid phase microextraction of refractory metals in environmental samples. Chemical Engineering Journal, 308: 169–176

Dong P, Liu W J, Wang S J, Wang H L, Wang Y Q, Zhao C C (2019). In suit synthesis of Fe$_3$O$_4$ on carbon fiber paper@polyaniline substrate as novel self-supported electrode for heterogeneous electro-Fenton oxidation. Electrochimica Acta, 308: 54–63

Dong S X, Dou X M, Mohan D, Pittman C U, Luo J M (2015). Synthesis of graphene oxide/schwertmannite nanocomposites and their application in Sb(V) adsorption from water. Chemical Engineering Journal, 270: 205–214

Du X, Qu F S, Liang H, Li K, Yu H R, Bai L M, Li G B (2014). Removal of antimony (III) from polluted surface water using a hybrid coagulation-flocculation-ultrafiltration (CF-UF) process. Chemical Engineering Journal, 254: 293–301

Duan C Y, Ma T Y, Wang J Y, Zhou Y B (2020). Removal of heavy metals from aqueous solution using carbon-based adsorbents: A review. Journal of Water Process Engineering, 37: 101339

Ganzoury M A, Chidiac C, Kurtz J, de Lannoy C F (2020). CNT-sorbents for heavy metals: Electrochemical regeneration and closed-loop recycling. Journal of Hazardous Materials, 393: 122432

Ghasemzadeh G, Momenpour M, Omidi F, Hosseini M R, Ahani M, Barzegari A (2014). Applications of nanomaterials in water treatment and environmental remediation. Frontiers of Environmental Science & Engineering, 8(4): 471–482

Guo W, Zhang Z, Wang H, Qin H, Fu Z (2021). Exposure characteristics of antimony and coexisting arsenic from multi-path exposure in typical antimony mine area. Journal of Environmental Management, 289: 112493

Guo X, Wu Z, He M, Meng X, Jin X, Qiu N, Zhang J (2014). Adsorption of antimony onto iron oxyhydroxides: adsorption behavior and surface structure. Journal of Hazardous Materials, 276: 339–345

Gusain R, Kumar N, Ray S S (2020). Recent advances in carbon nanomaterial-based adsorbents for water purification. Coordination Chemistry Reviews, 405: 213111

He M, Wang N, Long X, Zhang C, Ma C, Zhong Q, Wang A, Wang Y, Pervaiz A, Shan J (2019). Antimony speciation in the environment: Recent advances in understanding the biogeochemical processes and ecological effects. Journal of Environmental Sciences (China), 75: 14–39

He M, Wang X, Wu F, Fu Z (2012). Antimony pollution in China. The Science of the total environment, 421-422: 41–50

Hu X, Liu Y, Liu F, Jiang H, Li F, Shen C, Fang X, Yang J (2021). Simultaneous decontamination of arsenite and antimonite using an electrochemical CNT filter functionalized with nanoscale goethite. Chemosphere, 274: 129790

Huang D Y, Li B X, Wu M, Kuga S, Huang Y (2018). Graphene oxide-based Fe-Mg (hydr)oxide nanocomposite as heavy metals adsorbent. Journal of Chemical & Engineering Data, 63(6): 2097–2105

Huang T, Tang X Q, Luo K X, Wu Y, Hou X D, Tang S (2021). An overview of graphene-based nanoadsorbent materials for environmental contaminants detection. Trends in Analytical Chemistry, 139: 116255

Jiang H, Tian L, Chen P, Bai Y, Li X, Shu H, Luo X (2020). Efficient antimony removal by self-assembled core-shell nanocomposite of Co$_3$O$_4$@rGO and the analysis of its adsorption mechanism. Environmental Research, 187: 109657

Jiang S, Sun H, Wang H, Ladewig B P, Yao Z (2021). A comprehensive review on the synthesis and applications of ion exchange membranes. Chemosphere, 282: 130817

Khan N, Nawaz A, Islam B, Sayyad M H, Joya Y F, Islam S, Bibi S (2021). Evaluating humidity sensing response of graphene quantum dots synthesized by hydrothermal treatment of glucose. Nanotechnology, 32(29): 295504

Krishna Kumar A S, Jiang S J, Tseng W L (2015). Effective adsorption of chromium(VI)/Cr(III) from aqueous solution using ionic liquid functionalized multiwalled carbon nanotubes as a super sorbent. Journal of Materials Chemistry. A, Materials for Energy and Sustainability, 3(13): 7044–7057

Kroto H W, Heath J R, O'brien S C, Curl R F, Smalley R E (1985). C_{60}: Buckminsterfullerene. Nature, 318(6042): 162–163

Lee H J, Cho W, Oh M (2012). Advanced fabrication of metal-organic frameworks: template-directed formation of polystyrene@ZIF-8 core-shell and hollow ZIF-8 microspheres. Chemical communications (Cambridge, England), 48(2): 221–223

Leng Y Q, Guo W L, Su S N, Yi C L, Xing L T (2012). Removal of antimony(III) from aqueous solution by graphene as an adsorbent. Chemical Engineering Journal, 211–212: 406–411

Li F F, Long L Y, Weng Y X (2020a). A review on the contemporary development of composite materials comprising graphene/graphene derivatives. Advances in Materials Science and Engineering, 2020: 7915641

Li M, Liu Y, Shen C, Li F, Wang C C, Huang M, Yang B, Wang Z, Yang J, Sand W (2020). One-step Sb(III) decontamination using a bifunctional photoelectrochemical filter. Journal of Hazardous Materials, 389: 121840

Li X, Dou X, Li J (2012). Antimony(V) removal from water by iron-zirconium bimetal oxide: performance and mechanism. Journal of Environmental Sciences (China), 24(7): 1197–1203

Li Z Z, Shen C S, Liu Y B, Ma C Y, Li F, Yang B, Huang M H, Wang Z W, Dong L M, Wolfgang S(2020b). Carbon nanotube filter functionalized with iron oxychloride for flow-through electro-Fenton. Applied Catalysis B: Environmental, 260: 118204

Liu Y, Gao G, Vecitis C D (2020a). Prospects of an electroactive carbon nanotube membrane toward environmental applications. Accounts of Chemical Research, 53(12): 2892–2902

Liu Y, Liu F, Ding N, Shen C, Li F, Dong L, Huang M, Yang B, Wang Z, Sand W (2019a). Boosting Cr(VI) detoxification and sequestration efficiency with carbon nanotube electrochemical filter functionalized with nanoscale polyaniline: Performance and mechanism. The Science of the total environment, 695: 133926

Liu Y, Liu F, Qi Z, Shen C, Li F, Ma C, Huang M, Wang Z, Li J (2019b). Simultaneous oxidation and sorption of highly toxic Sb(III) using a dual-functional electroactive filter. Environmental pollution (Barking, Essex: 1987), 251: 72–80

Liu Y, Wu P, Liu F, Li F, An X, Liu J, Wang Z, Shen C, Sand W (2019c). Electroactive modified carbon nanotube filter for simultaneous detoxification and sequestration of Sb(III). Environmental Science & Technology, 53(3): 1527–1535

Liu Y B, Liu F Q, Ding N, Hu X M, Shen C S, Li F, Huang M H, Wang Z W, Sand W, Wang C C (2020b). Recent advances on electroactive CNT-based membranes for environmental applications: the perfect match of electrochemistry and membrane separation. Chinese Chemical Letters, 31(10): 2539–2548

Luo J, Luo X, Crittenden J, Qu J, Bai Y, Peng Y, Li J (2015). Removal of antimonite (Sb(III)) and antimonate (Sb(V)) from aqueous solution using carbon nanofibers that are decorated with zirconium oxide (ZrO_2). Environmental Science & Technology, 49(18): 11115–11124

Madannejad R, Shoaie N, Jahanpeyma F, Darvishi M H, Azimzadeh M, Javadi H (2019). Toxicity of carbon-based nanomaterials: Reviewing recent reports in medical and biological systems. Chemico-Biological Interactions, 307: 206–222

Maheshkumar K V, Krishnamurthy K, Sathishkumar P, Sahoo S, Uddin E, Pal S K, Rajasekar R (2014). Research updates on graphene oxide-based polymeric nanocomposites. Polymer Composites, 35(12):

2297–2310

Mishra S, Dwivedi J, Kumar A, Sankararamakrishnan N (2016). Removal of antimonite (Sb(III)) and antimonate (Sb(V)) using zerovalent iron decorated functionalized carbon nanotubes. RSC Advances, 6(98): 95865–95878

Mishra S, Sankararamakrishnan N (2018). Characterization, evaluation, and mechanistic insights on the adsorption of antimonite using functionalized carbon nanotubes. Environmental Science and Pollution Research International, 25(13): 12686–12701

Mobasherpour I, Salahi E, Ebrahimi M (2012). Removal of divalent nickel cations from aqueous solution by multi-walled carbon nano tubes: Equilibrium and kinetic processes. Research on Chemical Intermediates, 38(9): 2205–2222

Nasir A M, Goh P S, Abdullah M S, Ng B C, Ismail A F (2019). Adsorptive nanocomposite membranes for heavy metal remediation: Recent progresses and challenges. Chemosphere, 232: 96–112

Navarro P, Alguacil F J (2002). Adsorption of antimony and arsenic from a copper electrorefining solution onto activated carbon. Hydrometallurgy, 66(1–3): 101–105

Norra G F, Radjenovic J (2021). Removal of persistent organic contaminants from wastewater using a hybrid electrochemical-granular activated carbon (GAC) system. Journal of Hazardous Materials, 415: 125557

Pal M, Mondal M K, Paine T K, Pal P (2018). Purifying arsenic and fluoride-contaminated water by a novel graphene-based nanocomposite membrane of enhanced selectivity and sustained flux. Environmental Science and Pollution Research International, 25(17): 16579–16589

Pan M, Shan C, Zhang X, Zhang Y, Zhu C, Gao G, Pan B (2018). Environmentally friendly in situ regeneration of graphene aerogel as a model conductive adsorbent. Environmental Science & Technology, 52(2): 739–746

Ren S C, Ai Y J, Zhang X Y, Ruan M, Hu Z N, Liu L, Li J F, Wang Y, Liang J X, Jia H N, Liu Y Y, Niu D, Sun H B, Liang Q L (2020). Recycling antimony(III) by magnetic carbon nanospheres: turning waste to recoverable catalytic for synthesis of esters and triazoles. ACS Sustainable Chemistry & Engineering, 8(1): 469–477

Ren Y M, Yan N, Feng J, Ma J, Wen Q, Li N, Dong Q (2012). Adsorption mechanism of copper and lead ions onto graphene nanosheet/δ-MnO_2. Materials Chemistry and Physics, 136(2–3): 538–544

Saerens A, Ghosh M, Verdonck J, Godderis L (2019). Risk of cancer for workers exposed to antimony compounds: A systematic review. International Journal of Environmental Research and Public Health, 16(22): 4474

Salam M A, Mohamed R M (2013). Removal of antimony(III) by multi-walled carbon nanotubes from model solution and environmental samples. Chemical Engineering Research & Design, 91(7): 1352–1360

Saleh T A, Sarı A, Tuzen M (2017). Effective adsorption of antimony (III) from aqueous solutions by polyamide-graphene composite as a novel adsorbent. Chemical Engineering Journal, 307: 230–238

Sarkar B, Mandal S, Tsang Y F, Kumar P, Kim K H, Ok Y S (2018). Designer carbon nanotubes for contaminant removal in water and wastewater: A critical review. The Science of the total environment, 612: 561–581

Shahrin S, Lau W J, Goh P S, Ismail A F, Jaafar J (2019). Adsorptive mixed matrix membrane incorporating graphene oxide-manganese ferrite (GMF) hybrid nanomaterial for efficient As(V) ions removal. Composites. Part B, Engineering, 175: 107150

Shukla A K, Alam J, Alhoshan M, Dass L A, Ali F A A, Muthumareeswaran M R, Mishra U, Ansari M A (20 18). Removal of heavy metal ions using a carboxylated graphene oxide-incorporated polyphenylsulfone nanofiltration membrane. Environmental Science. Water Research & Technology, 4(3): 438–448

Su P D, Gao X Y, Zhang J K, Djellabi R, Yang B, Wu Q, Wen Z (2021). Enhancing the adsorption function of biochar by mechanochemical graphitization for organic pollutant removal. Frontiers of Environmental Science & Engineering, 15(6): 130

Thamer B M, Aldalbahi A, Moydeen A M, Al-Enizi A M, El-Hamshary H, El-Newehy M H (2019). Fabrication of functionalized electrospun carbon nanofibers for enhancing lead-ion adsorption from aqueous solutions. Scientific Reports, 9(1): 19467

Tripathy M, Padhiari S, Hota G (2020). L-cysteine-functionalized mesoporous magnetite nanospheres: synthesis and adsorptive application toward arsenic remediation. Journal of Chemical & Engineering Data, 65(8): 3906–3919

Vakili M, Qiu W, Cagnetta G, Huang J, Yu G (2021). Solvent-free mechanochemical mild oxidation method to enhance adsorption properties of chitosan. Frontiers of Environmental Science & Engineering, 15(6): 128

Vithanage M, Rajapaksha A U, Ahmad M, Uchimiya M, Dou X, Alessi D S, Ok Y S (2015). Mechanisms of antimony adsorption onto soybean stover-derived biochar in aqueous solutions. Journal of Environmental Management, 151: 443–449

Wan X, Huang Y, Chen Y (2012). Focusing on energy and optoelectronic applications: A journey for graphene and graphene oxide at large scale. Accounts of Chemical Research, 45(4): 598–607

Wang J T, Chen Y X, Zhang Z Q, Ai Y J, Liu L, Qi L, Zhou J J, Hu Z N, Jiang R H, Bao H J, Ren S C, Liang J X, Sun H B, Niu D, Liang Q L (2018a). Microwell confined iron oxide nanoparticles in honeycomb-like carbon spheres for the adsorption of Sb(III) and sequential utilization as a catalyst. ACS Sustainable Chemistry & Engineering, 6(10): 12925–12934

Wang L, Wang J Y, Wang Z X, Feng J T, Li S S, Yan W (2019). Synthesis of Ce-doped magnetic biochar for effective Sb(V) removal: performance and mechanism. Powder Technology, 345: 501–508

Wang L, Wang J Y, Wang Z X, He C, Lyu W, Yan W, Yang L (2018b). Enhanced antimonate (Sb(V)) removal from aqueous solution by La-doped magnetic biochars. Chemical Engineering Journal, 354: 623–632

Wang X X, Chen Z S, Yang S B (2015a). Application of graphene oxides for the removal of Pb(II) ions from aqueous solutions: experimental and DFT calculation. Journal of Molecular Liquids, 211: 957–964

Wang Y, Yang R, Li M, Zhao Z J (2015b). Hydrothermal preparation of highly porous carbon spheres from hemp (*Cannabis sativa* L.) stem hemicellulose for use in energy-related applications. Industrial Crops and Products, 65: 216–226

Wang Y Y, Ji H Y, Lu H H, Liu Y X, Yang R Q, He L L, Yang S M (2018c). Simultaneous removal of Sb(III) and Cd(II) in water by adsorption onto a MnFe$_2$O$_4$-biochar nanocomposite. RSC Advances, 8(6): 3264–3273

White B R, Stackhouse B T, Holcombe J A (2009). Magnetic gamma-Fe$_2$O$_3$ nanoparticles coated with poly-*L*-cysteine for chelation of As (III), Cu(II), Cd(II), Ni(II), Pb(II) and Zn(II). Journal of Hazardous Materials, 161(2–3): 848–853

Wilson S C, Lockwood P V, Ashley P M, Tighe M (2010). The chemistry and behaviour of antimony in the soil environment with comparisons to arsenic: A critical review. Environmental pollution (Barking, Essex: 1987), 158(5): 1169–1181

Xi J H, He M C, Wang K P, Zhang G Z (2015). Comparison of masking agents for antimony speciation analysis using hydride generation atomic fluorescence spectrometry. Frontiers of Environmental Science & Engineering, 9(6): 970–978

Xu C, Zhang B, Zhu L, Lin S, Sun X, Jiang Z, Tratnyek P G (2016). Sequestration of antimonite by zerovalent iron: using weak magnetic field effects to enhance performance and characterize reaction mechanisms. Environmental Science & Technology, 50(3): 1483–1491

Yang X, Zhou T, Ren B, Shi Z, Hursthouse A (2017). Synthesis, characterization, and adsorptive properties of Fe$_3$O$_4$/GO nanocomposites for antimony removal. Journal of Analytical Methods in Chemistry, 2017: 3012364

Yang X D, Wan Y S, Zheng Y L, He F, Yu Z, Huang J, Wang H, Ok Y S, Jiang Y, Gao B (2019). Surface functional groups of carbon-based adsorbents and their roles in the removal of heavy metals from aqueous solutions: A critical review. Chemical Engineering Journal, 366: 608–621

Yang X Z, Shi Z, Yuan M Y, Liu L S (2015). Adsorption of trivalent antimony from aqueous solution using graphene oxide: kinetic and thermodynamic studies. Journal of Chemical & Engineering Data, 60 (3): 806–813

Yang Y, Xiong Z, Wang Z, Liu Y, He Z J, Cao A K, Zhou L, Zhu L J, Zhao S F (2021). Super-adsorptive and photo-regenerable carbon nanotube based membrane for highly efficient water purification. Journal of Membrane Science, 621: 119000

Yap P L, Tung T T, Kabiri S, Matulick N, Tran D N H, Losic D (2020). Polyamine-modified reduced graphene oxide: A new and cost-effective adsorbent for efficient removal of mercury in waters. Separation and Purification Technology, 238(238): 116441

Yi G, Fan X F, Quan X, Chen S, Yu H T (2019). Comparison of CNT-PVA membrane and commercial polymeric membranes in treatment of emulsified oily wastewater. Frontiers of Environmental Science & Engineering, 13(2): 23

Yoo S H, Liu L, Park S (2009). Nanoparticle films as a conducting layer for anodic aluminum oxide template-assisted nanorod synthesis. Journal of Colloid and Interface Science, 339(1): 183–186

Yu H, He Y, Xiao G Q, Fan Y, Ma J, Gao Y X, Hou R T, Yin X Y, Wang Y Q, Mei X (2020). The roles of oxygen-containing functional groups in modulating water purification performance of graphene oxide-based membrane. Chemical Engineering Journal, 389: 124375

Yu T, Zeng C, Ye M, Shao Y (2013). The adsorption of Sb(III) in aqueous solution by Fe$_2$O$_3$-modified carbon nanotubes. Water science and technology: A journal of the International Association on Water Pollution Research, 68(3): 658–664

Yu T C, Wang X H, Li C (2014). Removal of antimony by FeCl$_3$-modified granular-activated carbon in aqueous solution. Journal of Environmental Engineering, 140(9): A4014001

Zeng G N, Hong C X, Zhang Y, You H Z, Shi W Y, Du M M, Ai N, Chen B (2020a). Adsorptive removal of Cr(VI) by sargassum horneri-based activated carbon coated with chitosan. Water, Air, and Soil Pollution, 231(2): 77

Zeng J Q, Qi P F, Shi J J, Pichler T, Wang F W, Wang Y, Sui K Y (2020b). Chitosan functionalized iron nanosheet for enhanced removal of As(III) and Sb(III): synergistic effect and mechanism. Chemical Engineering Journal, 382: 122999

Zhang B B, Song J L, Yang G Y, Han B X (2014). Large-scale production of high-quality graphene using glucose and ferric chloride. Chemical Science (Cambridge), 5(12): 4656–4660

Zhao D Y, Deng S B (2015). Environmental applications and implications of nanotechnologies. Frontiers of Environmental Science & Engineering, 9(5): 745

Zhou X X, Wang Y, Gong C C, Liu B, Wei G (2020). Production, structural design, functional control, and broad applications of carbon nanofiber-based nanomaterials: A comprehensive review. Chemical Engineering Journal, 402: 126189

Zhu K C, Duan Y Y, Wang F, Gao P, Jia H Z, Ma C Y, Wang C Y (2017). Silane-modified halloysite/Fe_3O_4 nanocomposites: simultaneous removal of Cr(VI) and Sb(V) and positive effects of Cr(VI) on Sb(V) adsorption. Chemical Engineering Journal, 311: 236–246

Zou J P, Liu H L, Luo J, Xing Q J, Du H M, Jiang X H, Luo X B, Luo S L, Suib S L (2016). Three-dimensional reduced graphene oxide coupled with Mn_3O_4 for highly efficient removal of Sb(III) and Sb(V) from water. ACS Applied Materials & Interfaces, 8(28): 18140–18149

Zou S J, Chen Y F, Zhang Y, Wang X F, You N, Fan H T (2021). A hybrid sorbent of α-iron oxide/reduced graphene oxide: studies for adsorptive removal of tetracycline antibiotics. Journal of Alloys and Compounds, 863: 158475